into account in the design and testing of power plants and other units and technological processes where there is gas–liquid flow in dynamic conditions.

NOTATION

$\bar{a}$, relative amplitude of pressure oscillations; p_1, p_2, p_3, pressure at different points of the pipeline; Δp_{3-1}, pressure difference; Q_1, liquid flow rate in pipeline 6; Q_2, liquid flow rate in pipeline 2; Q_2', liquid flow rate in measuring section; Q_2'', liquid flow rate in pipeline 5; ϕ, ϕ', actual relative volume gas content of flow in tests with and without pressure oscillations; ϕ_{eq}, ϕ_{eq}', equilibrium gas content of flow at mean pressure in the case of tests with and without pressure oscillations; $\Delta\phi$, additional gas liberation; ν, frequency of pressure oscillations.

LITERATURE CITED

1. É. V. Vengerskii, V. A. Morozov, and G. L. Usov, Hydrodynamics of Two-Phase Flows in Supply Systems of Power Plants [in Russian], Moscow (1982).
2. V. I. Petrov and V. F. Chebaevskii, Cavitation in High-Speed Rotary Pumps [in Russian], Moscow (1982).

HEAT TRANSFER IN CHANNELS WITH POROUS INSERTS DURING FORCED FLUID FLOW

A. A. Plakseev and V. V. Kharitonov

UDC 536.25:62-405.8

General analytic expressions are obtained to calculate heat transfer and temperature fields in a plane channel with a porous insert with allowance for the effective thermal conductivity of the heat carrier and the distribution of heat between the skeleton of the insert and the fluid in the boundary pores.

Porous media with various types of structures are finding increasing use in engineering to intensify the cooling of thermally-loaded objects when severe restrictions are placed on the temperature of the heat-transmitting surfaces. The studies [1-5] described methods of calculating the two-dimensional temperature distributions in a porous skeleton and in fluid moving through it. Convective heat transfer in a porous medium is usually described by using a system of equations based on two basic assumptions: 1) the Biot number for particles of the porous medium is small compared to unity; 2) all heat from the wall of the channel is transferred to the interior of the porous insert by conduction through the skeleton and is transmitted to the fluid by bulk heat transfer. Such an approximation is fully valid in the cases of the cooling of high-heat-conducting porous metals by water. If the thermal conductivity of the skeleton is negligible, then heat is transferred from the wall directly to the fluid moving in the boundary pores and is transferred into the interior of the porous layer by the effective thermal conductivity of the fluid due to its mixing in connected pores. This heat-transfer regime was studied in detail in [5, 6].

The laws governing heat transfer in the above-examined cases may differ considerably both qualitatively and quantitatively. Here, we propose a more general approach to calculating heat transfer in a channel with porous inserts: we consider the removal of heat from the wall by both the skeleton and the fluid and we examine the effect of the Biot number on bulk heat transfer. This problem is important for water-cooled structures made of steel, Invar, molybdenum, and other materials with pores and particles smaller than 1 mm when the thermal loads are approximately 10^6 W/m^2 or more. Most attention will be focused on the role of the effective thermal conductivity of the fluid and the heat distribution between the skeleton and the fluid in the formation of the temperature profiles and heat transfer in channels with porous inserts.

Moscow Physico-Engineering Institute.

Translated from Inzhenerno-Fizicheskii Zhurnal, Vol. 56, No. 1, pp. 36-44, January, 1988. Original article submitted July 31, 1987.

0022-0841/89/5601-0026 $12.50

TABLE 1. Effect of the Relative Heat Transfer α_f/α_s and Thermal Conductivity λ_f/λ_s of the Fluid on the Percentage of Heat η_0, %, Removed from the Channel Wall by the Skeleton on the Section of Stabilized Heat Transfer (calculated from Eq. (18))

α_f/α_s	λ_f/λ_s				
	0	0,1	1	10	∞
0	100	100	100	100	100
0,5	100	94	79	69	67
1	100	93	71	53	50
2	100	92	63	38	33
3	100	92	59	31	25
∞	100	91	50	9,1	0

Formulation of the Problem. We will examine a typical cooling system [4, 5]: a porous layer of thickness h (along the z axis) and length ℓ (along the x axis) is heated in the plane z = 0 by a heat flux q and is cooled by a one-phase heat carrier moving in a plane-parallel flow at the filtration velocity v along the x axis (perpendicular to the direction of the incident heat flow). The temperature of the fluid at the inlet (x = 0) is constant and equal to T_{in}. The bottom surface of the layer z = h is in contact with a thermally-insulated wall. The conductive heat transfer in the direction of fluid flow is negligible compared to the convective heat transfer [1-3]. The two-dimensional steady-state temperature distributions of the skeleton $T_s(x, z)$ and the fluid $T_f(x, z)$ satisfy the equations [1, 4, 5]:

$$\lambda_s \frac{\partial^2 T_s}{\partial z^2} - \alpha_v (T_s - T_f) = 0, \tag{1}$$

$$\lambda_f \frac{\partial^2 T_f}{\partial z^2} + \alpha_v (T_s - T_f) = \rho C_p v \frac{\partial T_f}{\partial x}. \tag{2}$$

Here, λ_s and λ_f are the transverse thermal conductivities of the porous skeleton and the fluid in the pores (with allowance for its mixing), respectively; α_v is the bulk heat-transfer coefficient for heat transfer between the skeleton and the fluid filtering through it. Let us formulate the boundary conditions. On the boundary between the porous layer and the heated wall, the heat delivered to the wall is redistributed: some of the heat η_0 is transmitted to the skeleton of the porous layer, while another portion $(1 - \eta_0)$ is transmitted from the wall directly to the fluid in the boundary pores (the pores having a common boundary with the wall). The part η_b supplied to the porous layer is transferred by conduction through the skeleton to the bottom wall. However, since this wall is thermally insulated, then this heat is returned to the porous layer directly into the fluid moving inside the boundary pores. These considerations lead to the boundary conditions:

$$T_f = T_{in} \quad \text{at} \quad x = 0; \tag{3}$$

$$-\lambda_s \frac{\partial T_s}{\partial z} = \eta_0(x) q, \quad -\lambda_f \frac{\partial T_f}{\partial z} = [1 - \eta_0(x)] q \quad \text{at} \quad z = 0; \tag{4}$$

$$-\lambda_s \frac{\partial T_s}{\partial z} = \lambda_f \frac{\partial T_f}{\partial z} = \eta_b(x) q \quad \text{at} \quad z = h. \tag{5}$$

Considering that the temperature of the bouundaries of the porous layer $T_s(x, 0)$, $T_s(x, h)$ coincides with the temperature of the wall in the given section x and that the temperature of the fluid in the boundary pores $T_f(x, 0)$, $T_f(x, h)$ differs from the temperature of the walls by the amount of the temperature head in the stagnant boundary layer of fluid, we can express the fractions of heat η_0 and η_b through the corresponding temperatures

$$1 - \eta_0(x) = \frac{\alpha_f (T_s - T_f)}{q} \quad \text{at} \quad z = 0; \tag{6}$$

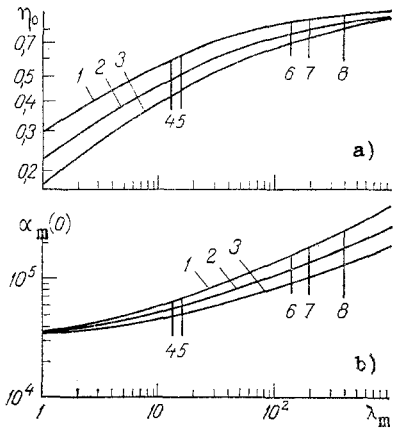

Fig. 1

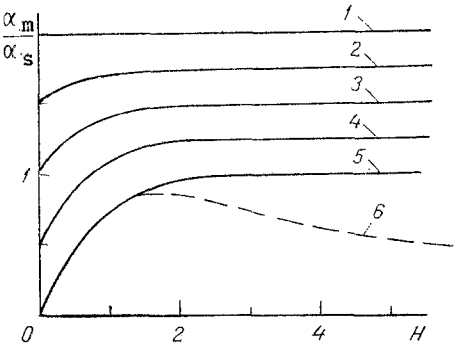

Fig. 2

Fig. 1. Effect of the thermal conductivity of the material of the porous skeleton and the hydraulic diameter of the pores on the fraction of heat removed from the wall by the skeleton (a) and on the local heat transfer of the wall (b) on the initial section with cooling of the porous layer by water at room temperature; calculation with Eqs. (12), (13) for a brush-like structure with the porosity $\Pi = 0.5$ at a hydraulic resistance of 10^7 Pa/m (1 atm/cm) and different hydraulic diameters: 1) $d_e = 0.5$ mm; 2) 1 mm; 3) 2 mm; material of the skeleton: 4) Invar; 5) steel 1Kh18N9T; 6) molybdenum; 7) aluminum; 8) copper. λ_m, W/(m·K); $\alpha_m(0)$, W/(m²·K).

Fig. 2. Dependence of the local heat transfer of a wall with a porous insert on the section of stabilized heat transfer on the relative thickness of the porous layer H with an effective thermal conductivity for the fluid $\lambda_f = \infty$ (curves 1-5) and $\lambda_f = 0$ (curve 6) and different values of ϕ: 1) $\phi = 1$; 2) 0.75; 3) 0.5; 4) 0.25; 5) $\phi = 0$; curves 1-5 were calculated with Eq. (13) or (16) at $\varkappa = 1$, while curve 6 was calculated from Eq. (17).

$$\eta_b(x) = \frac{\alpha_f (T_s - T_f)}{q} \quad \text{at} \quad z = h. \tag{7}$$

Here, α_f is the effective coefficient of heat transfer from the wall to the fluid in the boundary pores. Beyond the stagnant layer of fluid on the wall, characterized by the thermal resistance $1/\alpha_f$, heat is transmitted through the fluid to the interior of the porous layer thanks to mixing of the fluid. It should be noted that allowing for heat transfer by the moving fluid in the transverse direction (along the z axis) gives boundary-value problem (1-7) a mathematical singularity at the points of inflection (0,0) and (0,h), where conditions (3) and (4), (5) for T_f cannot be satisfied simultaneously. In fact, conditions (4) and (5) for T_f are realized outside the stagnant layer of fluid on the walls. Thus, we will henceforth require only the satisfaction of condition (3) at the points (0,0) and (0,h). This singularity has no effect on the temperature of the skeleton or its derivatives.

Boundary conditions (5) and (7) require further explanation. The fact that the bottom surface of the porous layer is in contact with a thermally insulated wall does not mean that we need to put $\partial T_s/\partial z = 0$ and $\partial T_f/\partial z = 0$ (at $z = h$) simultaneously. Conditions (5) and (7) mean that if the temperature of the bottom wall is higher than the temperature of the heat carrier in the boundary pores, then heat will inevitably be transferred directly from the wall to the fluid moving in the boundary pores. This fact is particularly noticeable when the skeleton is thin and bulk heat transfer is low. In this case, the temperatures of the top and bottom walls differ negligibly.

Thus, heat is transferred to the fluid not only as a result of its contact with the skeleton in the porous layer (which is reflected by the second terms in Eqs. (1) and (2)), but also by its contact with both walls of the layer through the boundary pores (i.e., from above and below). This means that the profile of fluid temperature may have a minimum near

TABLE 2. Comparison of Heat-Transfer Results Calculated from Eq. (13) with Experimental Data on the Heat Transfer of Walls with Projections at a Water Filtration Velocity v = 1.6 m/sec

Material of the projections	Spacing of the projections, mm	Size of the edge of a projection, mm	Porosity of the structure, %	Length of heated section, mm	$\alpha^{calc} \times 10^4$, W/(m²·K)	$\alpha^{expt} \times 10^4$, W/(m²·K)
Steel 1Kh18N9T	0.75	0.50	56	11.5	8.3	9 ±1
Duralumin D16T	0.80	0.57	49	20	17	16 ±2
Copper M1	1.40	0.90	59	12	17	18 ±2

the bottom wall (except for the inlet section, where the fluid temperature is assumed to be constant).

We find the local and effective heat transfer of the wall of a channel with a porous insert from the traditional formulas

$$\alpha_m(x) = \frac{q}{T_s(x, 0) - \bar{T}_f(x)}; \quad \alpha_{ef} = \frac{q}{\bar{T}_s(z=0) - T_{in}}, \tag{8}$$

where $\bar{T}_f(x) = \frac{1}{h}\int_0^h \bar{T}_f(x, z)dz$ is the fluid temperature averaged over the cross section of the porous layer; $\bar{T}_s(z = 0) = \frac{1}{\ell}\int_0^\ell T_s(x, 0)dx$ is the wall temperature averaged over the length of the porous layer.

It should be noted that Eqs. (1)-(8) are valid for porous inserts of any structure. The specific structure of the insert has an effect only on the value of the parameters λ_s, λ_f, α_v, and α_f and on the dependence of the last three parameters on the flow rate of the heat carrier. Recommendations for calculating these quantities for porous bodies with different structures are given in [5-10].

Temperature Distribution. At a given fluid flow rate and with known (and constant) thermophysical properties, including α_f and α_v, boundary-value problem (1-7) has an analytical solution which can be obtained in dimensionless form by using a finite Fourier transformation (see Appendix).

In the most general form, the resulting solution describes the two-dimensional temperature distribution of the skeleton and fluid and can be used to optimize the parameters of the porous layer, analyze the efficiency of its cooling, thermal deformation, etc. We should point out two features of the temperature distribution in the porous layer with a constant and unidirectional thermal load: 1) the fluid temperature averaged over the cross section of the layer increases in the flow direction in accordance with the linear law

$$\bar{T}_f(x) = T_{in} + \frac{qx}{\rho C_p v h}; \tag{9}$$

2) the transverse temperature profile of the skeleton at the inlet of the porous layer is expressed by hyperbolic functions

$$\theta_s(0, Z) = \frac{\eta_b}{\varphi}\operatorname{ch}(H - Z) + \eta_b \operatorname{sh}(H - Z), \tag{10}$$

where

$$\varphi = \alpha_f/\alpha_s \quad \alpha_s = \sqrt{\lambda_s \alpha_v}, \quad \eta_b(0) = \frac{\varphi}{(1+\varphi^2)\operatorname{sh} H + 2\varphi \operatorname{ch} H}. \tag{11}$$

We find from (3), (6), and (9) that

$$\eta_0(0) = \frac{\varphi + \operatorname{th} H}{2\varphi + (1+\varphi^2)\operatorname{th} H}. \tag{12}$$

Local heat transfer from the wall to the porous layer near the inlet

$$\alpha_m(0) = \alpha_s \frac{2\varphi + (1+\varphi^2)\operatorname{th} H}{1 + \varphi \operatorname{th} H}. \tag{13}$$

Given a sufficiently thick porous layer, when thH = 1, it follows that the conductivities are additive: $\alpha_m = \alpha_s(1 + \phi) = \alpha_s + \alpha_f$.

It can be seen that the temperature distribution of the skeleton and the heat transfer of the channel wall on the initial section are not explicitly dependent on the effective thermal conductivity of the fluid in the porous medium, since the temperature of the fluid at the inlet of the layer is independent of z in accordance with condition (3). It is not hard to show that Eqs. (11)-(13) are valie for any distance from the inlet if the effective thermal conductivity of the fluid is much greater than the thermal conductivity of the skeleton (the approximation $\lambda_f \to \infty$, see below). With a finite value of the ratio $\Lambda = \lambda_f/\lambda_s$, the length of the initial section where Eqs. (11)-(13) are valid is determined from the condition $X \ll 1/A_1$, where A_1 is the coefficient in the first exponent of the general solution (see Appendix). Thus, with $\lambda_f = 0$, we have $\mu_n = \pi n/H$, $A_1 + \mu_1^2/(1 + \mu_1^2)$ and $X_{ini.sc} \lesssim 1 + H^2/\pi^2$, i.e., the minimum length of the initial section $x_{ini.sc} \lesssim \delta_f$ at $H < 3$.

Effect of the Effective Thermal Conductivity of the Fluid on the Heat-Flow Distribution between the Skeleton and the Heat Carrier. If the thermal conductivity of the fluid can be ignored ($\lambda_f = 0$), then $\eta_0 = 1$, $\eta_b = 0$, $\phi = 0$, i.e., all of the heat goes from the heated wall to the skeleton, and there is no direct heat flow into the fluid either from the top (heated) or bottom (insulated) wall. The distribution of temperature and heat transfer in this case on the initial and stabilized sections was examined in detail in [9]. In particular, for the initial section – where heating of the fluid is small compared to the temperature head – we find from (13) that $\alpha_m(0) = \alpha_s thH$. This clearly illustrates the significance of the parameter $\alpha_s = \sqrt{\lambda_s \alpha_v}$ – the maximum possible heat-extraction capacity of the porous skeleton. Thus, for a copper skeleton at $\lambda_s = 200$ W/(m·K) and $\alpha_v = 2 \cdot 10^8$ W/(m³·K), we obtain $\alpha_s \approx 2 \cdot 10^5$ W/(m²·K). This is considerably greater than the heat transfer for tubes in the case of flow of liquid metals.

In the other limiting case ($\lambda_f/\lambda_s = \infty$), two variants are possible. If the thermal conductivity of the skeleton is low ($\lambda_s = 0$), then $\eta_0 = 0$, i.e., all heat is transferred from the wall directly to the fluid filling the boundary pores. In this case, it is important to consider the heat transfer α_f and the mixing of the fluid, as was done in [6]. If the effective thermal conductivity is high ($\lambda_f = \infty$), then the fractions of heat η_0 and η_b and the local heat transfer of the channel wall are determined by Eqs. (11)-(13), regardless of the length of the channel. The dimensionless temperatures of the skeleton and the heat carrier are determined in any section x by the expressions

$$\theta_s(X, Z) = \frac{X}{H} + \theta_s(0, Z); \quad \theta_f(X, Z) = \frac{X}{Z}, \tag{14}$$

where $\theta_s(0, Z)$ has the form (10). It can be seen that the temperatures of the skeleton and the fluid increase linearly in the flow direction.

In the case of a finite value of the ratio $\Lambda = \lambda_f/\lambda_s$, Eqs. (10)-(13) are valid for the initial section. We will therefore examine the section of stabilized heat transfer. Here, the fraction of heat removed from the wall by the skeleton and the local heat transfer are determined by the expressions

$$\eta_0 = \frac{\varphi[H(2+\Lambda) - \varphi] + (\Lambda + \varphi^2)\varkappa H \operatorname{th} \varkappa H + \varphi^2/\operatorname{ch} \varkappa H}{\Lambda \varkappa H [2\varphi\varkappa + (1 + \varphi^2\varkappa^2) \operatorname{th} \varkappa H]}; \tag{15}$$

$$\frac{\alpha_s}{\alpha_m} = \frac{1}{H(1+\Lambda)} + \frac{H}{3(1+\Lambda)} + \left[\frac{1}{\varkappa} - \frac{\varphi\varkappa}{H(1+\Lambda)}\right] \times$$

$$\times \frac{1 + \varphi\varkappa \operatorname{th} \varkappa H}{\varkappa^2 [2\varphi\varkappa + (1 + \varphi^2\varkappa^2) \operatorname{th} \varkappa H]} + \left[\frac{1}{\varkappa} - \frac{2\varphi\varkappa}{H(1+\Lambda)}\right] \frac{\operatorname{th} \varkappa H + \varphi\varkappa(1 - 1/\operatorname{ch} \varkappa H)}{\varkappa H (1+\Lambda)[2\varphi\varkappa + (1 + \varphi^2\varkappa^2) \operatorname{th} \varkappa H]} -$$

$$- \frac{\varphi}{\varkappa H (1+\Lambda)[2\varphi\varkappa + (1 + \varphi^2\varkappa^2) \operatorname{th} \varkappa H]}. \tag{16}$$

These expressions lead to simple asymptotes: 1) at $\Lambda = 0$ or $\phi = 0$, we have $\eta_0 = 1$,

$$\frac{1}{\alpha_m} = \frac{h}{3\lambda_s} + \frac{1}{h\alpha_v}, \tag{17}$$

i.e., the local thermal resistance of the porous layer consists of the serially connected thermal resistances of the skeleton $h/3\lambda_s$ and the stagnant layer on the surface of the skeleton (pores) $1/h\alpha_v$; 2) at $\Lambda = \infty$, we obtain (11)-(13), as on the initial section; 3) with a finite value of Λ, we obtain the following for a thick porous layer, when $\text{th}\varkappa H = 1$

$$\eta_0 = \frac{1 + \varphi/\varkappa\Lambda}{1 + \varphi\varkappa}, \tag{18}$$

$$\frac{\alpha_s}{\alpha_m} = \frac{1}{(1+\Lambda)}\left\{\frac{1}{H} + \frac{H}{3} + \frac{1}{1+\varphi\varkappa}\left[\frac{\Lambda}{\varkappa} + \frac{1}{\varkappa^2 H} - \frac{\varphi}{H\varkappa} - \frac{2\varphi}{(1+\Lambda)H^2}\right] - \frac{\varphi}{\varkappa H(1+\varphi\varkappa)^2}\right\}. \tag{19}$$

Table 1 illustrates the effect of the relative thermal conductivity of the fluid and heat transfer in the boundary pores on the value of η_0. It can be seen that the latter may be considerably less than unity. Only at $\alpha_f/\alpha_s < 0.3$ and $H > 1$-2 does the difference between the values of η_0 determined with $\lambda_f = 0$ and $\lambda_f = \infty$ not exceed 25%, since more than 75% of the heat from the wall is removed by the skeleton.

Figure 1 shows the effect of the thermal conductivity of the material of the porous skeleton on the percentage of heat η_0 removed from the wall by the skeleton. The effect of the thermal conductivity of the skeleton material on the local heat transfer of the wall α_m is also shown. It follows from Fig. 1 that the higher the thermal conductivity of the skeleton material, the greater the fraction of heat removed from the wall by the skeleton and the greater the heat transfer. Thus, replacing Invar (λ_m = 12 W/(m·K) by copper (λ_m = 400 W/(m·K) leads to an increase in η_0 from 0.5 to 0.85 and to an increase in heat transfer from $0.5\cdot10^5$ to $1.5\cdot10^5$ W/(m²·K) for a given skeleton structure and rate of water flow. A decrease in the hydraulic diameter of the pores (with a constant porosity) also leads to an increase in η_0 and α_m. It was assumed in the calculations of the curves for Fig. 1 that the heat transfer α on the surface of the rods of a brushlike structure and on the wall in an inter-rod space is the same, as was shown in [7, 8]. Thus, $\alpha_f = \alpha\Pi$, $\alpha_v = 4\Pi\alpha/d_e$, where Π is the porosity of the brushlike structure; $d_e = \Pi d/(1-\Pi)$ is the equivalent (hydraulic) diameter of the pores [5-8]. The effective thermal conductivity of the fluid was determined from the formula [6]: $\lambda_f \approx 0.1\rho C_p v_e d_e$, which gives $\lambda_f \approx 400$ W/(m·K) at $\text{Re}_e = v_e d_e/\nu = 10^3$.

In the example being examined here, $\alpha_f/\alpha_s = \sqrt{\alpha d_e \Pi/4\lambda_s}$ increases with an increase in the flow rate of the fluid (Reynolds number) approximately as $\text{Re}_e^{0.35}$, since the heat transfer of particles in the porous medium increases as $\text{Re}_e^{0.7}$ [7, 8]. In connection with the increase in the ratios α_f/α_s and λ_f/λ_s, an increase in the flow rate of the heat carrier is accompanied by a decrease in the fraction of heat extracted from the wall by the skeleton (Table 1).

Table 2 compares results on heat transfer calculated with Eq. (12) against experimental data on the heat transfer of walls of copper, duralumin, made with small projections [10]. The heat transfer on the surface of the square projections and on the wall between the projections was determined by the same method as for the cylindrical projections of a brushlike structure.

Figure 2 clearly illustrates the effect of the effective thermal conductivity of the fluid and the thickness of the porous layer on the local heat transfer of its wall for two limiting cases: $\lambda_f = \infty$ (curve 1-5) and $\lambda_f = 0$ (curve 6). It is evident that the difference between these curves is greater, the greater the amount of heat removed from the wall directly by the fluid through the boundary pores. If we ignore the heat-transfer component α_f (curve 5), as is customary, then we might introduce a large error into the calculation of heat transfer. This fact is most noticeable for small and large thicknesses of the porous layer.

Since the local heat transfer of the channel wall at $\lambda_f = \infty$ is the same at any distance from the inlet, then curves 5 and 6 in Fig. 2 represent the boundaries of the maximum scatter of heat transfer as a function of the effective thermal conductivity of the fluid. This range of α_m might be expanded considerably if allowance is made for α_f.

The above examples show that the distribution of the heat flow between the skeleton and the fluid in the boundary pores has a significant effect on the heat transfer of the walls of channels with porous inserts, particularly in the case of a skeleton with high porosity and low thermal conductivity and a high rate of flow of the heat carrier. Either Eq. (12) or (15) can be used for an approximate evaluation of η_0. When gases rather than liquids in

drop form are used as the heat carrier, the importance of the thermal conductivity of the skeleton increases greatly and, with a high degree of accuracy, we can put $\eta_0 = 1$.

Effect of the Biot Number on Bulk Heat Transfer. In a small Biot number approximation ($Bi = \alpha d/\lambda_m$, where λ_m is the thermal conductivity of the material of the projection and d is the diameter of the projection of the brushlike structure), we have $\alpha_v = \alpha S_v$, where S_v is the total surface of the pores calculated per unit volume of the porous layer. At Bi $\sim$ 1 or more, the temperature of the projection, averaged over its radius (for any z), is different than the temperature of its surface (for the same z). This temperature difference can be estimated by approximating the radial temperature distribution in the projection by a parabola. As a result, due to the internal thermal resistance of the projection in the radial direction, the bulk heat-transfer coefficient decreases in accordance with the expression

$$\alpha_v = \frac{\alpha S_v}{1 + \varphi \mathrm{Bi}}, \tag{20}$$

where ϕ is the form factor of the fin (a particle of the porous medium). Thus, $\phi = 1/8$ for a cylindrical projection and $\phi = 1/6$ for a plane fin.

It follows from Eq. (20) that the effect of the Biot number on the distribution of temperature and heat transfer in the porous layer is small up to Bi $\sim$ 1 (the values of α_v at Bi = 1 differ by no more than 17%).

APPENDIX

The solution of boundary-value problem (1)-(7) in dimensionless form:

$$\theta_s(X, Z) = \frac{T_s - T_{in}}{T_0} = \frac{X}{H} + \frac{C}{\varkappa^2}[\mathrm{ch}\,\varkappa(H-Z) + \varphi\varkappa\,\mathrm{sh}\,\varkappa(H-Z)] -$$

$$- D(\mathrm{ch}\,\varkappa Z + \varphi\varkappa\,\mathrm{sh}\,\varkappa Z) + \frac{6 - H^2 + 3(H-Z)^2}{6H(1+\Lambda)} - E +$$

$$+ \sum_{n=1}^{\infty} B_n e^{-A_n X}\left(\cos\mu_n Z + \frac{\varphi\varkappa^2}{\mu_n}\sin\mu_n Z\right),$$

$$\theta_f(X, Z) = \frac{T_f - T_{in}}{T_0} = \frac{X}{H} + C\left(\frac{1}{\varkappa^2} - 1\right)[\mathrm{ch}\,\varkappa(H-Z) +$$

$$+ \varphi\varkappa\,\mathrm{sh}\,\varkappa(H-Z)] - D(1-\varkappa^2)(\mathrm{ch}\,\varkappa Z + \varphi\varkappa\,\mathrm{sh}\,\varkappa Z) + \frac{6 - H^2 + 3(H-Z)^2}{6H(1+\Lambda)} -$$

$$- E - \frac{1}{H(1+\Lambda)} + \sum_{n=1}^{\infty} B_n(1+\mu_n^2)\, e^{-A_n X}\left(\cos\mu_n Z + \frac{\varphi\varkappa^2}{\mu_n}\sin\mu_n Z\right).$$

Here

$$A_n = \mu_n^2[\Lambda + 1/(1+\mu_n^2)]; \quad \varkappa^2 = (1+\Lambda)/\Lambda = 1 + \lambda_s/\lambda_f;$$

$$B_n = \frac{2}{\mu_n(H\mu_n^2 + 2\varphi\varkappa^2 + \varphi^2\varkappa^4 H)}\left\{\frac{\varphi\varkappa^2}{H\Lambda\mu_n(\varkappa^2+\mu_n^2)} \times\right.$$

$$\times\left[1 + \frac{\mu_n^2 + \varphi^2\varkappa^4}{\mu_n^2 - \varphi^2\varkappa^4}\cos\mu_n H\right] -$$

$$\left. - \frac{\varphi\mu_n\left(\mathrm{ch}\,H + \varphi\,\mathrm{sh}\,H + \frac{\mu_n^2 + \varphi^2\varkappa^4}{\mu_n^2 - \varphi^2\varkappa^4}\cos\mu_n H\right)}{\Lambda(1+\mu_n^2)(\mathrm{sh}\,H + 2\varphi\,\mathrm{ch}\,H + \varphi^2\,\mathrm{sh}\,H)} - \frac{\mu_n}{\Lambda(\varkappa^2+\mu_n^2)(1+\mu_n^2)}\right\};$$

$$C = \frac{1}{2\varphi\varkappa \operatorname{ch}\varkappa H + (1+\varphi^2\varkappa^2)\operatorname{sh}\varkappa H}\left[\frac{1}{\varkappa} - \frac{\varphi\varkappa}{H(1+\Lambda)}\right];$$

$$D = \frac{\varphi}{\varkappa H(1+\Lambda)[2\varphi\varkappa \operatorname{ch}\varkappa H + (1+\varphi^2\varkappa^2)\operatorname{sh}\varkappa H]};$$

$$E = \frac{(1-\varkappa^2)[\operatorname{sh}\varkappa H + \varphi\varkappa(\operatorname{ch}\varkappa H - 1)][H(1+\Lambda) - 2\varphi\varkappa^2]}{\varkappa^4 H^2(1+\Lambda)[2\varphi\varkappa \operatorname{ch}\varkappa H + (1+\varphi^2\varkappa^2)\operatorname{sh}\varkappa H]};$$

$$H = h/\delta_s, \quad Z = z/\delta_s, \quad T_0 = q\delta_s/\lambda_s,$$

$$\delta_s = \sqrt{\lambda_s/\alpha_v}, \quad X = x/\delta_f, \quad \delta_f = \rho v C_p/\alpha_v;$$

μ_n are roots of the transcendental equation $\tan \mu_n H = \frac{2\phi\varkappa^2\mu_n}{\mu_n^2 - \phi^2\varkappa^4}$.

The general form of the expression for calculating η_0:

$$\eta_{l0} = \frac{\operatorname{sh}\varkappa H + \varphi\varkappa \operatorname{ch}\varkappa H}{\varkappa^2[2\varphi\varkappa \operatorname{ch}\varkappa H + (1+\varphi^2\varkappa^2)\operatorname{sh}\varkappa H]} + \frac{1}{1+\Lambda}$$

$$- \frac{\varphi(\operatorname{sh}\varkappa H + \varphi\varkappa \operatorname{ch}\varkappa H - \varphi\varkappa)}{H(1+\Lambda)[2\varphi\varkappa \operatorname{ch}\varkappa H + (1+\varphi^2\varkappa^2)\operatorname{sh}\varkappa H]} - \varphi\varkappa^2 \sum_{n=1}^{\infty} B_n e^{-A_n X}.$$

LITERATURE CITED

1. S. N. Bugorskaya, A. G. Eliseev, Yu. A. Zeigarnik, et al., Heat Transfer and Thermal Strains in Cooled Multilayered Systems [in Russian], Moscow (1982), pp. 65-90.
2. V. A. Maiorov, V. M. Polyaev, L. L. Vasil'ev, and A. I. Kiselev, Inzh.-Fiz. Zh., 47, No. 1, 13-24 (1984).
3. V. A. Maiorov, V. M. Polyaev, and L. L. Vasil'ev, Inzh.-Fiz. Zh., 47, No. 2, 199-205 (1984).
4. V. I. Subbotin, V. V. Kharitonov, A. A. Plakseev, and S. V. Alekseev, Izv. Akad. Nauk SSSR, Énerg. Transp., No. 6, 94-101 (1984).
5. V. V. Kharitonov, Thermophysical Calculation of Laser Mirrors [in Russian], Moscow (1985).
6. V. V. Kharitonov, A. A. Plakseev, V. N. Fedoseev, and V. V. Voskoboinikov, Teplofiz. Vys. Temp., 25, No. 5, 954-961 (1987).
7. L. S. Kokorev, V. N. Fedeseev, V. V. Kharitonov, and V. V. Voskoboinikov, New Approach to Calculating Heat Transfer in Porous Media [in Russian], Preprint, MIFI, 024-86, Moscow (1986).
8. L. S. Kokorev, V. I. Subbotin, V. N. Fedoseev, et al., Teplofiz. Vys. Temp., 25, No. 1, 92-96 (1987).
9. S. B. Koshelev, A. A. Plakseev, and A. I. Miroshnichenko, Problems of Thermophysics in Nuclear Power Plants [in Russian], Moscow (1986), pp. 58-64.
10. Yu. A. Kuz'min, A. A. Plakseev, V. N. Fedoseev, et al., Problems of Thermophysics in Nuclear Power Plants [in Russian], Moscow (1986), pp. 64-69.